

# Filamentation of phase-modulated femtosecond laser pulse on kilometer-long paths in the turbulent atmosphere

S.A. Shlenov, V.Yu. Fedorov, and V.P. Kandidov

*International Laser Center, Moscow State University*

Received November 30, 2006

The effect of refractive index fluctuations on the filamentation of a subterawatt femtosecond pulse on kilometer-long path in the turbulent atmosphere is investigated. A novel method of numerical simulation of the pulse filamentation on a long atmospheric path is proposed. The method involves analytical solutions for the chirped pulse, propagating in the air. Detailed pattern of filamentation in the phase-modulated pulse at the distances more than one kilometer is given.

## Introduction

The phenomenon of filamentation of high-power laser pulses opens new, in principle, possibilities of developing novel approaches to atmospheric monitoring, such as the broadband sensing of gaseous constituents, laser induced fluorescence and emission spectroscopy of aerosols and pollutants.<sup>1</sup> Possibility of receiving the sensing signal from a distance of several kilometers is most interesting. At the same time, filamentation of spectrally limited terawatt pulses in the air starts, under real conditions, at the distances of 100 m and shorter<sup>2</sup> because of the pulse decay into many filaments due to the modulation instability of laser radiation with the high power density.<sup>3</sup> Small perturbations, causing the pulse instability in the atmosphere, may be initiated by both the initial fluctuations of the light field at the output of a femtosecond laser system and by the turbulent fluctuations of the refractive index of the air.<sup>4-7</sup>

It is just the spatial modulation instability of the intense light field in air that hampers the formation of filaments at a long distance from the emitting aperture. The modulation instability gives rise to small-scale self-focusing of the radiation and, as a consequence, to multiple filamentation of the pulse, which occurs at a much shorter distance than the global self-focusing of the pulse as a whole.<sup>8</sup>

To move the area of filamentation to kilometer-long distances, it is necessary to form the pulse, in which the initially low power density increases, as the pulse propagates to the preset distance. In this case, with the properly chosen parameters, one can expect that, at the initial part of the path, the pulse intensity will be too low for the small-scale self-focusing and the formation of multiple filaments therefore filamentation will start at a longer distance, as the pulse intensity will increase. The peak intensity of the pulse during its propagation in the medium can increase due to the time compression of the pulse (Fig. 1).

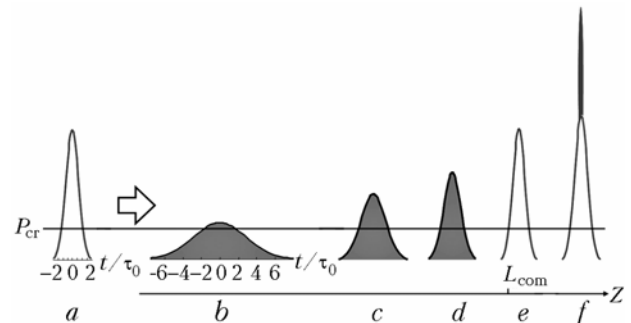


**Fig. 1.** Schematic of changes in the shape of a pulse with the negative initial phase modulation, propagating in the air at atmospheric pressure. Spectrally limited pulse (a); stretched pulse with the initial phase modulation (b); dispersion compression of a pulse upon its propagation in the air (c, d); formation of the spectrally limited pulse at the distance equal to the compression length  $L_{com}$  (e); shape of a pulse on its axis at filamentation in the absence of turbulence (f).

It should be noted that pulses of tens and hundreds femtosecond duration have a wide frequency spectrum and undergo marked dispersion spreading on extended atmospheric paths. At the same time, at the negative initial phase modulation of a pulse, it undergoes compression during the propagation in the atmosphere, since the gaseous constituents of air have normal dispersion of the group velocity at the wavelength of a Ti:Sapphire laser radiation.<sup>9</sup> Varying the phase modulation, it is possible to change the compression length of the pulse and thus to control the distance at which filamentation starts  $z_{fil}$ .

For the first time, the influence of the phase modulation on the formation of filaments was observed in Ref. 10. The experiments were carried out using collimated beams with the radius of 2.1 mm, energy of 6.2 mJ, and the width of the frequency spectrum, corresponding to the duration of the spectrally limited pulse of 250 fs. It has been found that the distance to the start of a filament

increased at detuning of the output compressor regardless of the sign of the initial phase modulation. In the following experiments on the pulse filamentation in air<sup>11</sup> precompensation for the dispersion of the group velocity has been used.

The field experiments<sup>1</sup> have clearly demonstrated the advantages of the phase-modulated pulses for the increase of the length of sensing using the supercontinuum, which is generated upon the kilometer-long filamentation. The propagation of phase-modulated pulses with the energy of 190 mJ was studied in detail in Ref. 12. Depending on the pulse modulation, the initial pulse duration  $\tau_{80}$  varied from 0.2 to 9.6 ps, which corresponded to the variation of the peak power in the range  $P_{80} = (190 \div 4)P_{cr}$ , where  $P_{cr}$  is the critical power of self-focusing. The longest distance, at which the authors succeeded to observe plasma channels, was achieved at the initial pulse duration  $\tau_{80} = 2.4$  ps and was equal to 370 m. The further increase of the phase modulation led to disappearance of plasma channels, although hot spots were observed in the distribution of the energy flux density up to the distances of 2 km.

The filamentation of the phase-modulated pulse with the Gaussian profile in a regular medium was studied theoretically in detail in Ref. 13. The influence of phase modulation of a pulse on its filamentation was found to be determined by two factors.

The first factor consists in the decrease of the peak power at the increasing duration of the initially spectrally limited pulse and does not depend on the sign of the phase modulation. Indeed, at the phase modulation, the pulse duration increases, the peak power  $P_{80}$  decreases, and the distance to the filament  $z_{fil}$  increases.

The second factor consists in the precompensation for the dispersion of the group velocity and depends on the sign of the phase modulation. During the propagation in the medium with the normal dispersion, a pulse with the negative phase modulation is compressed, and its peak power increases. It is shown that the longest filament length is achieved under the condition that the compression length of the phase-modulated pulse exceeds slightly its self-focusing length. In Ref. 14, the filamentation of a phase-modulated pulse with the power up to  $10P_{cr}$ , propagating in air to a distance of several tens of meters, has been considered numerically in the axisymmetric formulation.

In the case of long atmospheric paths, the filamentation of high-power phase-modulated pulses changes qualitatively. At long distances, the atmospheric turbulence exerts significant influence, which manifests itself in pulse-to-pulse fluctuations of the process of laser beam decay into multiple filaments, in wandering of the start of filamentation both in the plane perpendicular to the direction of propagation and along the path.<sup>5,15,16</sup>

This paper presents some results obtained numerically on the filamentation of a subterawatt

femtosecond pulse with the initial phase modulation on a kilometer-long path under the conditions of atmospheric turbulence. The analysis is carried out based on the original semianalytical method, allowing the numerical consideration of the propagation, nonlinear optical interaction, and filamentation of the phase-modulated laser pulse on long atmospheric paths to be done with high spatial resolution.

## Dynamic model of stochastic filamentation of a pulse with the initial phase modulation in the turbulent atmosphere

The stochastic model of propagation of a phase-modulated pulse through the atmosphere allows for such phenomena as diffraction, dispersion, Kerr self-focusing, defocusing in plasma channels induced by the pulse, as well as turbulent fluctuations of the atmospheric refractive index  $\tilde{n}$  [Refs. 4 and 5]. The equation for the complex amplitude of the electric field  $E(x, y, z, t)$  of the pulse has the form

$$2ik_0 \left( \frac{\partial}{\partial z} + \frac{1}{v_g} \frac{\partial}{\partial t} \right) E = \Delta_{\perp} E - k_0 k_{\omega}^* \frac{\partial^2 E}{\partial t^2} + \frac{2k_0^2}{n_0} [\Delta n_k(x, y, z, t) + \Delta n_p(x, y, z, t) + \tilde{n}(x, y, z)] E, \quad (1)$$

where  $k_0$  is the wave number;  $v_g$  is the group velocity;  $k_{\omega}^* = \partial^2 k / \partial \omega^2$ ,  $\omega$  is the central frequency of the pulse;  $n_0$  is the linear refractive index.

The change in the air refractive index due to the Kerr nonlinearity can be represented in the form

$$\Delta n_k(x, y, z, t) = \frac{1}{2} n_2 |E|^2, \quad (2)$$

where  $n_2 = 0.56 \cdot 10^{-22} \text{ m}^2/\text{W}$  is the coefficient of cubic nonlinearity of the atmospheric refractive index.<sup>17</sup> This value of the nonlinear refractive index corresponds to the critical power of self-focusing  $P_{cr} = 1.7 \text{ GW}$ . Equation (2) does not describe the delay of the contribution from the induced scattering at molecular rotational transitions, which can be taken into account either directly<sup>18</sup> or through the introduction of the effective nonlinearity coefficient for a short pulse.<sup>4</sup>

The changes of the refractive index in the air plasma at atmospheric pressure, induced by the laser pulse at the photoionization, can be expressed as follows:

$$\Delta n_p(x, y, z, t) = -\omega_p^2 / (2n_0 \omega^2), \quad (3)$$

where  $\omega_p^2(x, y, z, t) = 4\pi e^2 N_e(x, y, z, t) / m$  is the plasma frequency;  $e$  and  $m$  are the electron charge and mass;  $N_e$  is the concentration of free electrons, which is determined according to the kinetic equation:

$$\frac{\partial N_e}{\partial t} = R(|E|^2)(N_0 - N_e), \quad (4)$$

where  $N_0$  is the concentration of neutral molecules;  $R(|E|^2)$  is the ionization rate, which is calculated according to the Perelomov–Popov–Terent’ev (PPT) model.<sup>19</sup>

Atmospheric fluctuations of the refractive index  $\tilde{n}(x, y, z)$ , perturbing the light field in the beam cross section are responsible for the random nature of filamentation. The refractive index  $\tilde{n}(x, y, z)$  is described by use of a classical model of atmospheric turbulence with the modified von Karman spectrum of spatial fluctuations of the refractive index<sup>20</sup>:

$$F_n(\kappa) = 0.033C_n^2(\kappa^2 + \kappa_L^2)^{-11/6} \exp(-\kappa^2/\kappa_l^2), \quad (5)$$

which covers both the inertial and dissipative range. Here  $\kappa$  is the spatial frequency of fluctuations of the refractive index. The structure constant  $C_n^2$  characterizes turbulent fluctuations, while the constants  $\kappa_L = 2\pi/L_0$  and  $\kappa_l = 5.92/l_0$  characterize the lower and upper boundaries of spatial frequencies in the inertial range ( $L_0$  and  $l_0$  are the outer and inner scales of turbulence, respectively).

Fluctuations of  $\tilde{n}$  are simulated by a set of phase screens assuming that the random influence of the layer of turbulent medium on the light beam manifests itself at distances  $\Delta z$ , which are larger than the outer scale of turbulence  $L_0$  and the length of diffraction conversion of phase perturbations of the light field into the amplitude ones.<sup>21</sup> To simulate the random field of spatial fluctuations of the phase of light field  $\tilde{\phi}(x, y)$  on the screens, we used the spectral method,<sup>22</sup> modified in Ref. 23 in order to reconstruct the influence of large-scale fluctuations of the refractive index in the atmosphere. The application of the modified spectral method to the simulation of atmospheric turbulence is considered in detail in Ref. 5.

We considered the filamentation of a laser pulse with the Gaussian distribution of intensity over the beam cross section. The time profile of the pulse was also assumed Gaussian with the quadratic phase modulation, corresponding to the linear frequency modulation.<sup>9</sup> Thus, the complex amplitude of the light field  $E(x, y, z = 0, t)$  at the output of the laser system was specified in the form

$$E = E_0 \sqrt{\frac{\tau_0}{\tau_{\delta 0}}} \exp\left(-\frac{x^2 + y^2}{2a_0^2} - \frac{t^2}{2\tau_{\delta 0}^2} + i\frac{\delta t^2}{2}\right), \quad (6)$$

where  $a_0$  is the cross width of the pulse;  $\tau_{\delta 0}$  is the pulse duration;  $\delta$  is the phase modulation parameter. In Eq. (6), we have introduced the duration  $\tau_0$  and amplitude  $E_0$  of the spectrally limited pulse, which are acquired in the linear medium by the Gaussian pulse with the negative initial phase modulation  $\delta < 0$  at the compression length  $L_{\text{com}} = -\tau_0^2 \tau_{\delta 0}^2 \delta / |k_0^*|$ .

The dispersion length  $L_{\text{disp}} = \tau_0^2 / |k_0^*|$  of the spectrally limited pulse is a characteristic scale of the problem as well. The phase modulation parameter  $\delta$  can be

expressed through the duration of the spectrally limited  $\tau_0$  and the phase-modulated  $\tau_{\delta 0}$  pulses as follows:

$$\delta = -\sqrt{(\tau_{\delta 0}/\tau_0)^2 - 1} / \tau_{\delta 0}^2. \quad (7)$$

The duration  $\tau_{\delta 0}$  and the parameter  $\delta$  of the pulse also can be expressed through the introduced parameters  $L_{\text{disp}}$  and  $L_{\text{com}}$ :

$$\tau_{\delta 0} = \tau_0 \sqrt{1 + (L_{\text{com}}/L_{\text{disp}})^2}; \quad \delta = -\frac{L_{\text{com}}}{\tau_{\delta 0}^2 L_{\text{disp}}}. \quad (8)$$

## Problems in numerically simulating the filamentation on long atmospheric paths

Numerical simulation of filamentation of a high-power femtosecond laser pulse on long atmospheric paths takes very long computer time, because the range of characteristic scales of laser radiation significantly extends upon the nonlinear optical transformation of the pulse. During the propagation of a high-power pulse, a filament with the characteristic scale of  $10^{-2}$  cm is formed in air. The fine structure of variations for the phase of the light field in the filament has the scale on the order of  $10^{-3}$  cm. Thus, as the pulse with the radius of several centimeters propagates in air, the range of spatial scales of variation of the light field in the plane of the cross section  $XOY$  extends by three orders of magnitude.

To resolve the fine structure of the filament, about ten nodes are needed on the characteristic scale of phase variation, and the step of the computational grid  $h$  in the plane  $XOY$  should be of the order of 10  $\mu\text{m}$ . At the same time, in simulating the beam propagation in the free space, the range of variation of coordinates in the transverse plane should be rather wide and equal to about 10 radii of the initial beam. In field experiments, pulses with the diameter of several centimeters are used, and the computational area may amount to 10–50 cm. As a result, about  $10^4$ – $10^5$  nodes are needed for each coordinate in the plane  $XOY$ , and the total number of nodes of the computational grid in this plane achieves  $10^8$ – $10^{10}$ .

To diminish the size of data arrays to be processed, we use a specialized computational grid with a variable step in the plane  $XOY$  (see Ref. 24). The area of the pulse cross section is divided into two zones. In the first zone, lying near the pulse axis, where the pulse energy is concentrated, the grid step  $h$  is chosen small and constant to reconstruct adequately spatial variations of the light field phase. In the second zone, lying in the pulse periphery, the step increases slowly with the distance from the axis. The computational grid with the variable step in the plane of the beam cross section allows the four- to five-fold reduction of the program execution time to be achieved.

The decrease of the characteristic scale of perturbations of the light field in the plane  $XOY$  inevitably results in the reduction of the integration step of the problem  $\Delta z$  along the evolution coordinate  $z$ , coinciding with the direction of pulse propagation. Indeed, the splitting procedure, which is usually used in numerical solution of Eq. (1), requires for the step  $\Delta z$  to be no longer than the diffraction length for the smallest scale of variation of the light field in the plane  $XOY$ . At the characteristic scale of variation of the field in the filament equal to  $10^{-2}$  cm, the integration step  $\Delta z$  along the direction of pulse propagation at the wavelength  $\lambda = 0.8 \mu\text{m}$  does not exceed 10 cm. Under conditions of strong nonlinear optical interaction between the radiation and laser induced plasma, the step  $\Delta z$  decreases adaptively with the increase of the nonlinear phase shift. As a result, the number of steps on a kilometer-long path along the direction of pulse propagation exceeds  $10^5$ .

Finally, to reconstruct adequately the changes in the pulse envelope and the process of generation of laser plasma upon filamentation, a rather short time step  $\Delta t$  is needed. The step  $\Delta t$  should be no longer than  $10^{-2}$  of the pulse duration, while the size of the time domain of computations should be no smaller than three to five pulse durations. At the phase modulation, the initial pulse duration increases several times and the number of nodes of the time computational grid achieves  $10^3$ – $10^4$ .

In general, the filamentation of the phase-modulated pulse on a kilometer-long atmospheric path is described by the nonlinear optical stochastic problem with the dimensionality of  $(3D + 1)$ . According to the above estimates, the simulation of this problem requires for processing numerical arrays with the total size of  $10^{16}$ – $10^{19}$ , and the search for efficient methods for numerical investigation of this problem is quite urgent. This search can be performed in two directions.

First, it is the use of high-performance computer systems and code parallelization algorithms for optimal loading. An original algorithm of parallel computations on clusters for the investigation of pulse filamentation was proposed in Refs. 25 and 26.

Another direction consists in the development of simple physical models for the study of particular problems within the phenomenon of filamentation of laser pulses. For the problem of filamentation of a phase-modulated pulse at an extended path in the turbulent atmosphere, we propose here and justify physically a semianalytical model, which allows a significant reduction of the computation time to be achieved.

### Semianalytic model of filamentation of the phase-modulated pulse in the turbulent atmosphere

Having undergone phase modulation a pulse takes longer duration  $\tau_{\delta 0}$ , while its peak power,  $P_{\delta 0}$ , becomes lower as compared to the corresponding

parameters  $\tau_0$  and  $P_0$  of the spectrally limited pulse of the same energy. At  $P_{\delta 0}$  close to the critical power of self-focusing  $P_{cr}$ , the distance to the filamentation zone increases significantly. This increase depends, to a high extent, on the compression of the phase-modulated pulse, during which the pulse duration  $\tau_{\delta}(z)$  decreases and the peak power  $P_{\delta}(z)$  increases with the distance  $z$ . In particular, at  $P_{\delta 0} < P_{cr}$  the filamentation of the pulse is possible only due to the pulse compression in air. Quite an extended part of the atmospheric path, where the peak intensity of the phase-modulated pulse  $I_{\delta}(z)$  is much lower than the photoionization threshold of the gaseous constituents of the air, can be called the prefilamentation zone:

$$I_{\delta}(z \leq z_{\text{prefil}}) \ll I_{cr}, \quad (9)$$

where  $z_{\text{prefil}}$  is the boundary of the prefilamentation zone;  $I_{cr}$  is the photoionization threshold.

In the prefilamentation zone, the energy changes in the pulse are determined by the Kerr self-focusing and by fluctuations of the refractive index in the turbulent atmosphere, which lead to the spatial redistribution of the power density in the plane, perpendicular to the direction of propagation, as well as by the compression, which causes redistribution of power over time within the pulse, so that the power from the leading and trailing edges of the pulse is concentrated near its center, thus increasing the value  $P_{\delta}(z)$ . If in the prefilamentation zone ( $z < z_{\text{prefil}}$ ) the changes in the intensity at the Kerr self-focusing and the power in time layers at compression are relatively small, then the transformation of the pulse in space and time can be considered independently. This approximation is equivalent to application of the method of splitting physical factors to Eq. (1) for the complex amplitude of the field. Since there is no photoionization in the prefilamentation zone, after the splitting of Eq. (1) the chain of equations for the complex amplitude of the light field in the pulse takes the form

$$2ik_0 \frac{\partial E_{\text{sp}}}{\partial z} = \Delta_{\perp} E_{\text{sp}} + \frac{2k_0^2}{n_0} [\Delta n_k(x, y, z, t) + \tilde{n}(x, y, z)] E_{\text{sp}}, \quad (10)$$

$$2ik_0 \frac{\partial E_{\text{time}}}{\partial z} = -k_0 k'_0 \frac{\partial^2 E_{\text{time}}}{\partial t^2}. \quad (11)$$

In a turbulent atmosphere, the spatial modulation instability and the formation of multiple filaments in the high-power pulse develop at shorter distances than the global self-focusing of the pulse as a whole with the formation of a single filament. Thus, the spatial changes in the phase of the light field due to the Kerr nonlinearity and fluctuations of the refractive index are decisive as compared to changes due to the self-modulation in the Kerr medium. This allows us to neglect the phase self-modulation in the prefilamentation zone and to consider the pulse compression in the linear approximation. As a result the chain of equations (10) and (11) breaks, which otherwise should be solved successively at each elementary integration

step  $\Delta z$  along the path according to the splitting method. For Eq. (11), describing the compression of the Gaussian pulse in the linear medium, an analytical solution is known,<sup>9</sup> which determines that the time shape of the pulse  $T(z, t)$  changes with the distance  $z$ :

$$T(z, t) = \frac{E_{\text{time}}(z, t)}{E_0} = \sqrt{\frac{\tau_0}{\tau_\delta(z)}} \exp\left\{-\frac{t^2}{2\tau_\delta^2(z)} + i\varphi(z, t)\right\}, \quad (12)$$

where  $\varphi(z, t)$  is the known phase of the pulse.<sup>9</sup>

Since in Eq. (10), describing the spatial transformation of the pulse in the beam cross section, the time  $t$  is a parameter, the solution of this equation  $E_{\text{sp}}(x, y, z, t)$  can be presented in the multiplicative form as follows:

$$E_{\text{sp}}(x, y, z, t) = T(z, t)\tilde{A}(x, y, z). \quad (13)$$

The function  $\tilde{A}(x, y, z)$  that describes the change of the complex amplitude of the light field in the beam cross section with the distance, obeys the stochastic equation:

$$2ik_0 \frac{\partial \tilde{A}(x, y, z)}{\partial z} = \Delta_\perp \tilde{A}(x, y, z) + \frac{2k_0^2}{n_0} [\Delta n_k (|E_{\text{sp}}|^2) + \tilde{n}(x, y, z)] \tilde{A}(x, y, z). \quad (14)$$

Equation (13) along with Eqs. (12) and (14) forms the semianalytic model, describing the prefilamentation of the pulse. Physically, the approximations accepted in the model mean that, in the prefilamentation zone, the pulse keeps the Gaussian shape (12) in the entire  $XOY$  plane and the phase self-modulation is absent. The Gaussian profile of the pulse preserves despite the spatial perturbations of the field in this plane due to the atmospheric turbulence and Kerr nonlinearity. This representation is acceptable, because the atmospheric turbulence is stationary during the femtosecond pulse, and the nonlinear phase self-modulation due to the Kerr nonlinearity is local in the pulse cross section being significant only in the vicinity of incipient filaments. In the model constructed, the compression of the pulse during its propagation manifests itself in the power redistribution between time layers of the pulse. According to Eqs. (12) and (13), the change of the power  $P(z, t)$  in the pulse time layers with the distance is described by the dependence

$$P(z, t) = P_{\delta 0} \frac{\tau_{\delta 0}}{\tau_\delta(z)} \exp\left\{-\frac{t^2}{\tau_\delta^2(z)}\right\}. \quad (15)$$

With this energy redistribution in time, the intensity at the center of the pulse  $I_\delta(x, y, z, t = 0)$  increases

and the contribution from the Kerr nonlinearity [Eq. (2)] to the variation of the refractive index increases as well:

$$\Delta n_k(x, y, z, t = 0) = \frac{1}{2} n_2 \frac{\tau_0}{\tau_\delta(z)} \exp\left\{-\frac{t^2}{\tau_\delta^2(z)}\right\} |\tilde{A}(x, y, z)|^2. \quad (16)$$

Equation (14) for the function of spatial change of the field  $\tilde{A}(x, y, z)$  is stationary. Its solution is the spatial distribution of the field, valid for all time layers of the pulse. The central layer ( $t = 0$ ), in which the power is maximum ( $P(z, t = 0) = P_\delta(z)$ ), determines the beginning of filamentation. Due to the spatial modulation instability of the light field, the stochastic formation of nonlinear focuses occurs in this layer, followed by the generation of hot spots of future filaments. Equation (14) with the random field of the refractive index is integrated by use of the model of phase screens<sup>5</sup> to the boundary of the prefilamentation zone, defined as a distance  $z_{\text{prefil}}$ , at which the intensity in hot spots is twice as high as the initial peak intensity  $I_0$  of the spectrally limited pulse. The complex amplitude at the boundary of the prefilamentation zone can be presented in the form

$$\tilde{E}(x, y, z_{\text{prefil}}, t) = T(z_{\text{prefil}}, t) \tilde{A}(x, y, z_{\text{prefil}}), \quad z < z_{\text{prefil}}. \quad (17)$$

The field  $\tilde{E}(x, y, z_{\text{prefil}}, t)$  is random due to fluctuations of the refractive index along the atmospheric path.

Beyond the prefilamentation zone  $z > z_{\text{prefil}}$ , the field at hot spots increases very fast with the distance. In the vicinity of hot spots, the contributions from the plasma nonlinearity and phase self-modulation become significant, and the deviation of the pulse profile from the Gaussian one and the change of the field  $\tilde{E}(x, y, z, t)$  are described by the initial equation (1) along with Eqs. (2)–(4). The initial condition for this problem is the field  $\tilde{E}(x, y, z_{\text{prefil}}, t)$  [Eq. (17)], obtained at the boundary of the prefilamentation zone. The (3D + 1) system of equations is solved with the use of a computer cluster, for which an original parallelization algorithm based on the splitting method as applied to the diffraction problem has been developed.

To analyze the accuracy of the semianalytical method developed, we have considered the test problem about the self-focusing of a Gaussian phase-modulated pulse in the absence of fluctuations of the refractive index of the air. The test problem was solved at  $\tilde{n} = 0$  and  $\Delta n_p = 0$  taking into account the dispersion of the group velocity both by the semianalytic method [Eqs. (12) and (14)] and through the direct integration of Eq. (1). The pulse with the following parameters was considered: energy  $W = 6.1$  mJ, the initial radius of the beam

$a_0 = 2$  cm, spectrally limited duration  $\tau_0 = 100$  fs, wavelength  $\lambda = 0.8$   $\mu\text{m}$ , the coefficient  $k_0''$ , determining the dispersion of the group velocity, was taken equal to  $0.16$   $\text{fs}^2/\text{cm}$ . For these parameters, the peak intensity was  $I_0 = 2.7$   $\text{GW}/\text{cm}^2$  and the peak power was  $P_0 = 34.3$   $\text{GW}$ , which was 20 times higher than the critical power of self-focusing in air at the atmospheric pressure. At the initial phase modulation, the pulse duration increased up to 727 fs, corresponding to the compression length  $L_{\text{com}} = 4500$  m, the peak intensity and power amounted to, respectively,  $I_{80} = 0.38$   $\text{GW}/\text{cm}^2$  and  $P_{80} = 4.7$   $\text{GW}$ .

Figure 2 depicts the peak intensity  $I_\delta(z)$  of the pulse as a function of the path length  $z$ . The slow increase of the intensity at the beginning of propagation, caused by the pulse compression and Kerr self-focusing at  $P_{80}/P_{\text{cr}} \approx 2.7$ , gives place to the avalanche growth while approaching the plane of nonlinear focusing. The distance to this plane can be considered as a distance to the start of filamentation  $z_{\text{fil}}$  in the regular air medium.

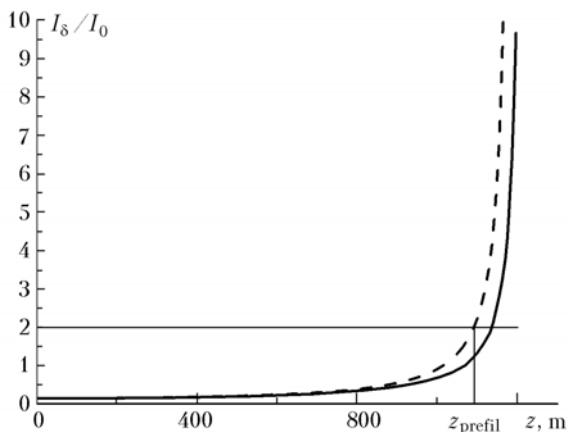


Fig. 2. Peak intensity  $I_\delta(z)$  of a pulse vs. path length  $z$ : (solid curve) numerical solution of Eq. (1), (dashed curve) semianalytic method.

One can see that the semianalytic method underestimates the distance  $z_{\text{fil}}$  as compared to the result of direct integration of Eq. (1). The analysis, carried out at different pulse parameters, shows that the systematic error of the semianalytic method, estimated by  $z_{\text{fil}}$ , does not exceed 10%.

## Evolution of a phase-modulated pulse along the path

The semianalytic method developed has been applied to numerical investigation of the filamentation of a subterawatt femtosecond pulse of different power, duration, and initial phase modulation on long paths in the turbulent atmosphere. The horizontal path was considered assuming constant parameters of atmospheric turbulence with the inner scale  $l_0 = 3$  mm and the outer scale  $L_0 = 10$  m. The structure constant ranged within

$C_n^2 = (0.2-0.4) \cdot 10^{-15} \text{cm}^{-2/3}$ . The maximum path length achieved 3 km.

As an example, we considered the phase-modulated pulse with the same parameters as in the previous section. It should be noted that the distance to the beginning of filamentation  $z_{\text{fil}}$ , spectrally limited by the pulse, in the absence of turbulence ( $C_n^2 = 0$ ) amounts to 320 m.

According to the semianalytic method, to obtain a realization of the light field  $\tilde{E}(x, y, z, t)$  at pulse filamentation in the turbulent atmosphere, we first considered the prefilamentation zone, at which the random field  $\tilde{E}_{\text{sp}}(x, y, z, t)$  was represented in the multiplicative form [Eq. (13)]. In this representation, the random function  $\tilde{A}(x, y, z)$ , describing the change of the light field in the pulse cross section, was determined by the numerical solution of Eq. (14) using the model of phase screens. The deterministic time profile  $T(z, t)$  of the pulse was specified by Eq. (12). Then, at the path leg, where the filamentation develops, equation (1) was directly integrated numerically with the field  $\tilde{E}_{\text{sp}}(x, y, z_{\text{prefil}}, t)$ , obtained at the boundary of the prefilamentation zone as the initial condition. The solution of Eq. (1), which takes into account the diffraction, dispersion, phase self-modulation, self-focusing in the Kerr medium, and, finally, defocusing in the induced laser plasma, yielded the realization of the field  $\tilde{E}(x, y, z, t)$  on a long path.

Figure 3 depicts the intensity  $\tilde{I}_\delta(x, y, z, t = 0)$  in the central time layer of the phase modulated pulse at different distances along the path. At the beginning of the prefilamentation zone ( $z < 700$  m), the Kerr self-focusing is weakly pronounced, because the peak power  $P_\delta(z)$  only slightly exceeds the critical power of self-focusing. Fluctuations of the phase of the light field at random variations of the refractive index in the turbulent atmosphere lead to redistribution of the power over the beam cross section. Local intensity maxima are formed in some regions of the cross section. At the end of the prefilamentation zone ( $z = 1030$  m), these maxima begin to increase due to the spatial modulation instability of the intense light field in air, and at  $z = 1380$  m the intensity at one of them achieves  $5 \cdot 10^9$   $\text{W}/\text{cm}^2$ .

Within the path leg, where the filamentation of the pulse develops ( $z \geq 1400$  m), the maximum with the highest intensity grows like an avalanche, forming the so-called "hot" spot in the pulse cross section.<sup>27</sup> The intensity at the hot spot achieves the multiphoton ionization threshold at the distance  $z_{\text{fil}} = 1490$  m, corresponding to the beginning of a filament. The defocusing in the laser induced plasma leads to restriction of the growth and then to a decrease of the intensity in the central pulse layer. The aberration nature of the plasma defocusing causes then the formation of a ring structure, surrounding the filament ( $z = 1520$  m).

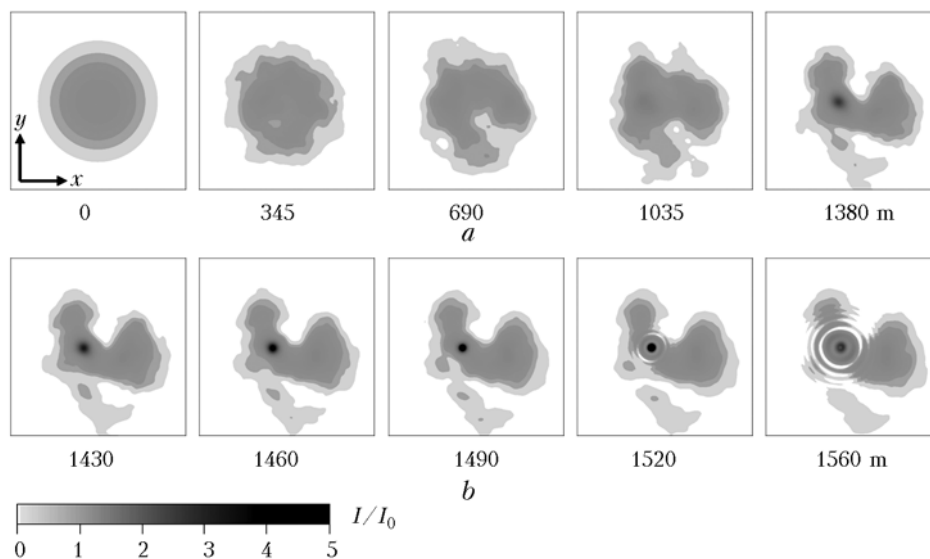


**Fig. 3.** Intensity  $\tilde{I}_\delta(x, y, z, t = 0)$  in the central time layer of the phase-modulated pulse with the energy  $W = 6$  mJ and duration  $\tau_{80} = 727$  fs at different distances  $z$ ; compression length  $L_{\text{com}} = 4500$  m: (a) prefilamentation zone, (b) filamentation zone.

It should be noted that along with the “hot” spot, the filament is formed from, the intensity profile includes other hot spots, but the power in their vicinity is still insufficient for the formation of a filament.

The development of a “hot” spot from the maximum, formed at the prefilamentation zone, can be considered as self-focusing of an individual perturbation in the pulse cross section. Assume that the maximum has the Gaussian profile, and, before the formation of a filament with the intensity equal to the photoionization threshold, it evolves independently of its environment. Then, from the random realization of the intensity  $I_\delta(x, y, z_{\text{prefil}}, t = 0)$  in the central time layer at the prefilamentation boundary, we can determine for this maximum the effective radius  $a_{\text{loc}}$  and the power  $P_{\text{loc}}$ , concentrated within the circle with this radius. According to the Marburger’s equation,<sup>28</sup> valid for collimated beams with the Gaussian profile, we can find the self-focusing distance  $z_{\text{loc}}$  for the selected maximum:

$$z_{\text{loc}} = \frac{0.367k_0 a_{\text{loc}}^2}{\left\{ \left[ \left( \frac{P_{\text{loc}}}{P_{\text{cr}}} \right)^{1/2} - 0.852 \right] - 0.0219 \right\}^{1/2}}. \quad (18)$$

Summing up  $z_{\text{loc}}$ , calculated by Eq. (18), over the distance to the prefilamentation boundary  $z_{\text{prefil}}$ , we obtain the estimate of the distance to the beginning of the filament  $z_{\text{fil}}^{\text{estim}}$ .

In the case under consideration, the boundary of the prefilamentation zone is  $z_{\text{prefil}} = 1400$  m. The maximum with the highest intensity at this distance has the effective radius  $a_{\text{loc}} = 0.44$  cm and carries the power  $P_{\text{loc}} = 3.3$  GW, equal to 1.9 of the critical

power of self-focusing. The self-focusing distance  $z_{\text{loc}}$ , calculated by Eq. (18) for the maximum with such parameters, is equal to 108 m. Thus, we obtain the estimate of the distance to the beginning of the filament  $z_{\text{fil}}^{\text{estim}} = 1508$  m which deviates from  $z_{\text{fil}} = 1490$  m obtained numerically, by 1.2%. It follows from the above analysis that, from the calculated prefilamentation of the phase-modulated pulse in the turbulent atmosphere, one can estimate the distance to the start of filamentation quite accurately.

In the applied problems on the filamentation of high-power femtosecond laser pulses in the atmosphere, the transport of the laser energy at long distances plays an important role. In this connection, it is interesting to study the influence of the increase in the pulse energy on the process of filamentation under turbulent conditions. We have considered the pulse with the same time ( $\tau_0 = 100$  fs,  $\tau_{80} = 727$  fs,  $L_{\text{com}} = 4500$  m) and spatial ( $a_0 = 2$  cm) parameters, but with the doubled energy ( $W = 12$  mJ). In this case, the peak intensity of the phase-modulated pulse increased up to  $I_{80} = 0.8 \cdot 10^9$  W/cm<sup>2</sup>, the peak power increased up to  $P_{80} = 5.5P_{\text{cr}}$ , and the distance  $z_{\text{fil}}$  to the formation of the filament shortened to 772 m. However, despite the increase of the pulse energy, only one filament formed at this distance, as in the previous case.

For both of the pulses considered, the compression length  $L_{\text{com}}$  was 4500 m. However, the filament was formed at much shorter distances ( $z_{\text{fil}} = 1500$  m for the pulse with low energy and  $z_{\text{fil}} = 772$  m for the pulse with high energy). In both cases, the compression of the phase-modulated pulse in time was not used efficiently for the localization of the laser energy.

Indeed, the compression length  $L_{\text{com}}$ , at which the maximum compression is achieved due to the linear dispersion of the phase-modulated pulse in air, far exceeds the distance to the formation of a filament, and, consequently, the contribution of the linear dispersion to the nonlinear growth of the intensity is small.

To increase the contribution of the linear dispersion, we considered the pulse with energy of 6 mJ, decreasing the compression length to 3000 m. In this case, the duration of the phase-modulated pulse  $\tau_{80}$  amounted to 490 fs, its peak intensity was  $I_{80} = 0.56 \cdot 10^9 \text{ W/cm}^2$ , and the peak power was  $P_{80} = 4.1P_{\text{cr}}$ . The numerical simulation of the dynamic problem on the filamentation of this pulse has shown that the filament was formed at the distance  $z_{\text{fil}} = 931 \text{ m}$ . Thus, the increase of the contribution from the linear dispersion through shortening of the compression length of the phase-modulated pulse leads to shortening of the distance to the formation of a filament from 1500 m to 931 m.

The higher concentration of power in time can be achieved by decreasing the duration  $\tau_0$  of the spectrally limited pulse. We considered the pulse with the duration  $\tau_0 = 50 \text{ fs}$  and energy  $W = 3 \text{ mJ}$  at the phase modulation, when the compression length was  $L_{\text{com}} = 3000 \text{ m}$  and the duration increased to  $\tau_{80} = 960 \text{ fs}$ . The peak power  $P_{80}$  at this phase modulation of the pulse is close to  $P_{\text{cr}}$ , which is insufficient for the formation of a filament only due to the Kerr self-focusing. The growth of the intensity at the linear dispersion of the pulse is responsible for the decisive contribution to the initiation of a filament in this case. This is confirmed by the results of numerical simulation, according to which the filament in the pulse considered is formed at the distance  $z_{\text{fil}} = 2935 \text{ m}$ , which is close to the compression length  $L_{\text{com}}$ . However, as in the previous cases, only one filament was formed.

All the examples considered indicate that, in the turbulent atmosphere, only one filament is formed in the pulse with the initial phase modulation regardless of the pulse energy and the modulation parameter. At the same time, at the end of the prefilamentation zone, where "hot" spots begin to form in the pulse cross section, the peak power of the pulse  $P_{\delta}(z_{\text{prefil}})$  far exceeds the critical power of self-focusing, amounting to 4–13 $P_{\text{cr}}$ , depending on the values of the parameters.

The absence of multiple filaments in the high-power phase-modulated pulse in the case of long atmospheric paths is explained by the spatial selection of the modulation instability of the intense light field in the air. Indeed, for a hundreds meters long prefilamentation zone, the light field in the pulse cross section is perturbed. The characteristic scale of the perturbations covers a wide range, corresponding to the power spectrum of atmospheric turbulence. Therefore, as the intensity increases in the

process of the dispersion compression of the pulse, there always is such a perturbation, which has the largest growth increment.

The concentration of the power in the filament, being developed from this perturbation, suppresses the generation of other filaments in the pulse. This competition between the formed filament and incipient ones becomes stronger because of the turbulent broadening of the pulse, due to which the intensity in the pulse cross section decreases.

The results of numerical simulation, considered above, are in a qualitative agreement with the experimental data,<sup>12</sup> in which the authors failed to observe plasma channels at the increased pulse duration upon the introduction of the phase modulation.

## Conclusions

1. The semianalytic method has been proposed for the investigation of filamentation of a high-power femtosecond laser pulse with the initial phase modulation for the case of long paths in the turbulent atmosphere. The method is based on the multiplicative representation of the light field in the prefilamentation zone, in which its spatial variation is determined by fluctuations of the refractive index and by the Kerr nonlinearity of the air, while the temporal variation is determined by the pulse compression in the linear dispersive medium. Further on the path, where the phase self-modulation of the field and the nonlinearity of the laser plasma become significant, the problem on the filamentation of the pulse with random perturbations, induced in the prefilamentation zone, is solved numerically. The method significantly reduces the computation time for the investigation of the formation of filaments and plasma channels in femtosecond laser pulses for kilometer-long paths in the turbulent atmosphere.

2. The initial phase modulation of the high-power femtosecond pulse allows the distance to the start of the filamentation in the turbulent atmosphere to be increased by several times. At the same time, only one filament is formed in the pulses considered regardless of their energy and the compression length. This is a consequence of the spatial selectivity of the modulation instability of the intense light field with the turbulence-induced perturbations during the propagation in the air as a medium with the Kerr nonlinearity.

## Acknowledgements

This study was supported, in part, by the Russian Foundation for Basic Research (Grant No. 06-02-08004).

## References

1. J. Kasparian, M. Rodriguez, G. Mejean, J. Yu, E. Salmon, H. Wille, R. Bourayou, S. Frey, Y.-B. Andre, A. Mysyrowicz, R. Sauerbrey, J.-P. Wolf, and L. Woste, *Science* **301**, No. 5629, 61–64 (2003).



2. S.L. Chin, S.A. Hosseini, W. Liu, Q. Luo, F. Theberge, N. Akozbek, A. Becker, V.P. Kandidov, O.G. Kosareva, and H. Schroeder, *Can. J. Phys.* **83**, 863–905 (2005).
3. V.I. Bespalov, A.G. Litvak, and V.I. Talanov, *Nonlinear Optics* (Nauka, Novosibirsk, 1968), pp. 428–463.
4. K.Yu. Andrianov, V.P. Kandidov, O.G. Kosareva, S.L. Chin, A. Talebpour, S. Petit, W. Liu, A. Iwasaki, and M.-K. Nade, *Izv. Ross. Akad. Nauk. Ser. Fiz.* **66**, No. 8, 1091–1102 (2002).
5. S.A. Shlenov and V.P. Kandidov, *Atmos. Oceanic Opt.* **17**, No. 8, 565–570 (2004).
6. M. Mlejnek, M. Kolesik, J.V. Moloney, and E.M. Wright, *Phys. Rev. Lett.* **83**, No. 15, 2938–2941 (1999).
7. L. Berge, S. Skupin, F. Lederer, G. Mejean, J. Yu, J. Kasparian, E. Salmon, J.P. Wolf, M. Rodriguez, L. Woste, R. Bourayou, and R. Sauerbrey, *Phys. Rev. Lett.* **92**, No. 22, 225002 (2004).
8. V.P. Kandidov, O.G. Kosareva, S.A. Shlenov, N.A. Panov, V.Yu. Fedorov, and A.E. Dormidonov, *Quant. Electron.* **35**, No. 1, 59–64 (2005).
9. S.A. Akhmanov, V.A. Vysloukh, and A.S. Chirkin, *Optics of Femtosecond Laser Pulses* (Nauka, Moscow, 1988), 312 pp.
10. S.L. Chin, “A study of the fundamental science underlying the transport of intense femtosecond laser pulses in the atmosphere,” Final Report for Grant No. DAAG55-97-1-0404 (1999).
11. H. Wille, M. Rodriguez, J. Kasparian, D. Mondelain, J. Yu, A. Mysyrowicz, R. Sauerbrey, J.P. Wolf, and L. Woste, *Eur. Phys. J. AP* **20**, 183–190 (2002).
12. G. Mechain, C. D’Amico, Y.-B. Andre, S. Tzortzakis, M. Franco, B. Prade, A. Mysyrowicz, A. Couairon, E. Salmon, and R. Sauerbrey, *Opt. Commun.* **247**, 171–180 (2005).
13. I.S. Golubtsov, V.P. Kandidov, and O.G. Kosareva, *Quant. Electron.* **33**, No. 6, 525–530 (2003).
14. R. Nuter and L. Berge, *J. Opt. Soc. Am. B* **23**, No. 5, 874–884 (2006).
15. V.P. Kandidov, O.G. Kosareva, M.P. Tamarov, A. Brode, and S. Chin, *Quant. Electron.* **29**, No. 10, 911–916 (1999).
16. S.L. Chin, A. Talebpour, J. Yang, S. Petit, V.P. Kandidov, O.G. Kosareva, and M.P. Tamarov, *Appl. Phys. B* **74**, 67–76 (2002).
17. E.T.J. Nibbering, G. Grillon, M.A. Franco, B.S. Prade, and A. Mysyrowicz, *J. Opt. Soc. Am. B* **14**, No. 3, 650–660 (1997).
18. M. Mlejnek, E.M. Wright, and J.V. Moloney, *Opt. Lett.* **23**, No. 5, 382–384 (1998).
19. A.M. Perelomov, V.S. Popov, and M.V. Terent’ev, *Zh. Eksp. i Teor. Fiz.* **50**, No. 5, 1393–1409 (1966).
20. V.E. Zuev, V.A. Banakh, and V.V. Pokasov, *Optics of the Turbulent Atmosphere* (Gidrometeoizdat, Leningrad, 1988), 270 pp.
21. S.S. Chesnokov, V.P. Kandidov, S.A. Shlenov, and M.P. Tamarov, *Proc. SPIE* **3432**, 14–25 (1998).
22. L.I. Mirkin, M.A. Rabinovich, and L.P. Yaroslavskii, *Zh. Vychisl. Mat. i Mat. Fiz.* **12**, No. 5, 1353–1357 (1972).
23. E.M. Johansson and D.T. Gavel, *Proc. SPIE* **2200**, 372–383 (1994).
24. V.P. Kandidov and V.Yu. Fedorov, *Quant. Electron.* **34**, No. 12, 1163–1168 (2004).
25. A.E. Bezborodov and S.A. Shlenov, *Izv. Ross. Akad. Nauk. Ser. Fiz.* **70**, No. 9, 1246–1250 (2006).
26. S.A. Shlenov, A.E. Bezborodov, and A.V. Smirnov, in: *Conference on Parallel and Distributed Processing Techniques and Applications (PDPTA’06)* (Las Vegas, NV, 2006), 1. PDP-4003, pp. 94–98.
27. S.A. Shlenov and V.P. Kandidov, *Atmos. Oceanic Opt.* **17**, No. 8, 571–575 (2004).
28. J.H. Marburger, *Prog. Quant. Electr.* **4**, 35–110 (1975).